Thesis for the Degree of Master of Science

Experimental investigation of an airbag inflation

by

Erik Lindén



Division of Fluid Dynamics
Department of Applied Mechanics
Chalmers University of Technology

Göteborg, Sweden, 2006

Abstract

Resistance- and hot wire technology has been applied to measure temperature and velocity of the gas generated during an airbag inflation. A cylindrical extension has been used between the gas generator and the bag, with the purpose of providing a measuring section. The temperature experienced by the resistance wire is assumed to be stagnation temperature and was found to reach maximum temperatures around 600 to 700 $^{\circ}C$ for all gas generators tested. The measured temperature was used to correct the hot wire signal to just be valid for velocity. Pressure has been measured to give information about the density and mass flow changes. From the signals observed unsteady shockwave analyze has been applied. The temperature change over the initial shock wave has been converted to other physical property changes, such as pressure, density, velocity and mass flow. The theory showed a very good agreement with the measured pressure. Unpredictable behavior was experienced in both the hot wire and resistance wire in the first 20 ms which could not be fully out explained. The signal from the hot wire was difficult to convert to velocity in higher temperatures than it was calibrated for.

Contents

1 Introduction **5**

2 Theory of compressible flow **7**

3 Measurement techniques **9**

4 Hot/Resistance wire theory **13**
4.1 The CTA technique 13
4.2 The CCA technique 13
4.3 Heat transfer of wires 14
4.4 Frequency response of wires 15
4.5 Choice of wire material 17

5 Calibration **21**
5.1 Calibration device 21
5.2 Probe manufacturing 23
5.3 Calibration of Hot wire 23
5.4 Calibration of Resistance wire 26

6 Experiment procedure **29**

7 Results and analysis **33**
7.1 Temperature measurements 33
7.2 Time response 35
7.3 Comparison with compressible flow theory 37
7.4 Hot wire measurements 41
7.5 Analysis of the first milliseconds 44

8 future work **47**

Bibliography **49**

Chapter 1

Introduction

Autoliv is a world leading automotive safety company. One of their most popular product is the inflatable restraint system which consist of a gas generator and a bag. In order to estimate the inflation characteristics numerical simulations are in use. But the lack of proper input values to the models, experiments of the inflations are necessary. The tank test method is the most used method when characterizing gas generators. It contains a gas generator in a sealed tank and a pressure sensor register the pressure. The disadvantage with this method is that it does not give useful property changes over time, instead it gives just a final state when the gas generation is over and from that a average value of the mass flow could be obtained.

The aim of this project was to measure physically time resolved quantities on the gas, generated during an air bag inflation, trying to characterize them. The specified quantities to measure were temperature and mass flow. The advantage with the chosen measurement technique should be that the measurements will end up in time series.

An airbag inflation is a very fast event where properties are assumed to change drastically over a wide range therefore it has been kept in mind when searching for measurement method that the time response of the measure technique has to be very fast. Another critical factor in the flow is the soot which can cause damage of a eventually probe inserted. A further consequence of the fast flow sequence is that it could create shocks. These shocks could probably cause problem for sensitive instruments or sensors.

The gas generator (also called inflator) is the device which produces the gas. They could be either pyrotechnic, gas generated by combustion of propellants, or they could contain pressurized gas or it could be a mixture of a pyrotechnic and a pressurized gas technique called hybrid inflator where the combustion generated gas mixes with the pressurized gas. In this project measurements were only done for the pyrotechnic one which mostly produces nitrogen gas.

Chapter 2

Theory of compressible flow

The gas generator inflation is considered as a simplified case where you can think that the gas is held at high pressure inside the gas generator. Suddenly an artificial wall vanish and the gas immediately flows out. Effects of friction on hole walls and the gas generation sequence are neglected in this simplification. The flow case can then be analyzed as a simplified unsteady one dimensional compressible flow, where the high pressure difference causes a shock propagating forward and induces a velocity of the gas behind. The difference to the stationary case is that the thermodynamic properties change not only in space but also in time, and an important consequence of that is that stagnation properties are not constant over the shockwave. The property changes over the shockwave can be found assuming calorically perfect gas, which implies that the internal energy, $h = c_p T$ and $\rho = P/RT$. The governing equations are valid for both the stationary and the non stationary wave motion case since the governing equations are defined relative to the shockwave, Anderson (1990).

To relate the thermodynamic properties over a shockwave the continuity, momentum and energy equation has to be studied. For the one dimensional flow case they reduce to equations 2.1 ,2.2 and 2.3.

$$\rho_1 u_1 = \rho_2 u_2 \tag{2.1}$$

$$P_1 + \rho_1 u_1^2 = P_2 + \rho_2 u_2^2 \tag{2.2}$$

$$h_1 + u_1^2/2 = h_2 + u_2^2/2 \tag{2.3}$$

Where h is the enthalpy, u is the velocity, P is the pressure and ρ is the density. After some algebraic work they will end up in the Hugoniot equation which in turn can be derived to temperature, density and pressure ratios across the shockwave. Below the temperature and density ratio as a function of the pressure ratio are shown, equ. 2.4 and 2.5 .

$$\frac{T_2}{T_1} = \frac{P_2}{P_1}\left(\frac{\frac{\gamma+1}{\gamma-1} + \frac{P_2}{P_1}}{1 + \frac{\gamma+1}{\gamma-1}\frac{P_2}{P_1}}\right) \tag{2.4}$$

$$\frac{\rho_2}{\rho_1} = \frac{1 + \frac{\gamma+1}{\gamma-1}\left(\frac{P_2}{P_1}\right)}{\frac{\gamma+1}{\gamma-1} + \frac{P_2}{P_1}} \tag{2.5}$$

Let us now derive u_p, the induced velocity behind the shock wave in the unsteady wave motion case, which is going to be measured.

Consider the case relative to the wave when the wave is propagating forward with a certain speed W in a still medium, the speed of the medium in front of it would propagate towards the shock wave with the speed, W. Behind the shock wave the speed of the medium would then be the difference between the speed of the wave and the induced speed due to the shock. Therefore u_1 and u_2 in the equations 2.1 - 2.3 will be replaced by W and $W - u_p$, see figure 2.1. The speed of the propagating wave then becomes as

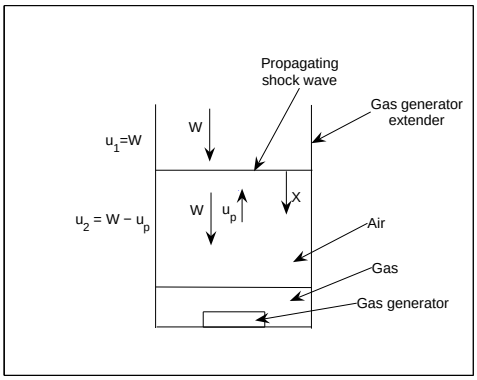


Figure 2.1: Unsteady wave motion

equation 2.6, a detailed derivation of this equation can be found in section 7.2 in Anderson (1990).

$$W = a_1\sqrt{\frac{\gamma+1}{2\gamma}\left(\frac{P_2}{P_1} - 1\right) + 1} \tag{2.6}$$

Here a_1 is the sound of speed in front of the shock wave. Using equ. 2.1 and 2.6, u_p can be found to be:

From equation 2.1 u_p can be solved by rewriting it to equation 2.7.

$$u_p = \frac{a_1}{\gamma}\left(\frac{P_2}{P_1} - 1\right)\left(\frac{\frac{2\gamma}{\gamma+1}}{\frac{P_2}{P_1} + \frac{\gamma-1}{\gamma+1}}\right)^{1/2} \tag{2.7}$$

Chapter 3

Measurement techniques

To measure in a very extreme flow, with varying temperature, velocity and the fluid itself (for instance soot generated), the constraints make it difficult to find a proper measurement technique.

As one temperature measurement sensor, thermocouple could be an alternative choice. It contains of two dissimilar electrically conducting materials coupled at an interface Childs (2001). A conductor transfer heat from the warmer side to the colder side in the same direction electrical charge carriers moves within the material. If the circuit can be complete the charge carriers can be used to create an electrical current and a voltage. When two dissimilar conductors are used a net current flow is generated in the direction of the flow of the most conductive material. The voltage generated depends on two things, the temperature difference and the properties of the conductors. If an ice bath (zero degrees reference) is used as the colder junction the voltage output will refer to the temperature in Celsius degrees (Tellurex Corporation). In order to have a fast time response the junction should be very thin due to the thermal inertia. Nowadays there are fast thermocouple available on the market, some company have presented thermocouple with a time constant of one millisecond but its purpose is mainly to measure temperature at the wall, so there is a doubt if it would manage to reach the same fast response in a flow.

However, there is another temperature measurement technique where the time response depends on the thermal inertia, namely the cold wire or resistance wire. But in this case the temperature is observed from the resistance change when the a constant current is running through the wire. The relation ship is as follows, Childs (2001):

$$R_T = R_0(1 + \alpha_0(T - T_0)) \tag{3.1}$$

As for the thermocouple the time response gets faster when the thickness of the temperature sensor reduces and the speed of the flow increases. As an example, a 2.0 μm tungsten wire at 60 ms the 3dB frequency response is calculated to around 2500 Hz, see figure 4.3.

An attempt to decrease the time response could be to use two hot wires running at different overheat ratios. Hot-wire is mainly a measurement tool for turbulent velocities. Since the wire is heated to a temperature significantly higher then the flow, the heat

transfer to the wire also depends on the velocity of the flow which has a cooling effect. With two hot wires having different calibration functions depending on both temperature and velocity and placed parallel close to each other so that they observe the same flow properties the temperature and the velocity should be able to get. The benefit is that the temperature observations will have the same fast response as the velocity observations due to the feed back amplifier, Bruun (1995).

A similar technique is the Aspirating probe technique which also take care of compressible effects. The probe also contain two hot wire running at different speeds, but they are placed in a channel. This conveys that it will bring information about the pressure. The idea is that you know that the channel is choked at the exit ($M = 1$) thus the continuity equation becomes as equation 3.2.

$$\rho U = \left(\frac{P_0}{\sqrt{T_0}}\right)\sqrt{\frac{\gamma}{R}}\left(1+\frac{2}{\gamma+1}\right)^{(\gamma+1)/2(\gamma-1)} \tag{3.2}$$

If the mass flow is uniform in the channel an area quota could be added on the right hand side in equation 3.2 so the equation is valid for where the probe is placed in the channel. Considering Kings law which is the commonly used relation for heat transfer of a wire running with a constant temperature anemometry. The Kings law could be written as a function of pressure and temperature, see equation 3.3, Ng & Epstein (1983).

$$E^2 = \left[A + B\left(\frac{P_T}{\sqrt{T_T}}\right)^n\right](T_w - T_T) \tag{3.3}$$

Another method where you also take care of the pressure is when you calibrate the dual hot wire also for pressure having the probe in a pressure chamber in front of a jet flow Sigfrids (2003).

So far only analog temperature measurement methods has been presented. To get a further improvement of the temperature measurement considering time response and accuracy laser technology should be taken into account. Spontaneous Rayleigh and Raman scattering is the absorption and re-mission of electromagnetic radiation by atoms and molecules. In the scattering technique you need a spectrometer to detect the light and a laser to excite the particles in the flow. Rayleigh scattering is elastic scattering of light by molecules or particles less then one μm in size. When a molecule is promoted incident from the ground state to a higher unstable vibrational state and returned to its original state it is classed as Rayleigh scattering. Rayleigh scattering has the disadvantages that you must know the individual concentrations of the species in the flow and it can also be prejudiced by other processes in the flow. If the molecule return to another vibrational state instead of the ground state it is classed as Raman scattering Childs (2001).

A non-linear Raman scattering technique is the so called CARS (Coherent Anti-stokes Raman Scattering), it is non-linear considering the scattering signal to the laser intensity. Therefore a laser with very high intensity is needed. the probe volume is created by three

laser beams and the Raman resonances probed are pure rotational. (Sean P.Kearney.....) Very high Resolution has been obtained by CARS, E. K. Gustafson & Byer (????) presented a resolution of 100 MHz in their CARS set up for their super sonic jet experiment. Compare to Rayleigh scattering CARS has the advantages to measure in particulate laden flows.

All optic methods named until now has been for one point. The Laser-induced fluorescence technique is an two-dimensional temperature measurement technique. Laser-induced fluorescence (LIF) is the optical emission from molecules that have been excited to higher energy levels by the absorption of laser radiation Childs (2001).

Other techniques that are more of mapping character of the flow are Absorption and emission spectroscopy technique, Infrared thermometry where the difficulty is to measure in a 3d flow, however they give a good thermal distribution picture of the flow. To get a good idea what happens in the flow support a simple photographic method could be used.

The Schlieren method is a visualization technique which can observe possible shocks and flow motions and it has its advantages that it does not need as much light as it would require if a common photographing was used.

When the decision of measurement technique was made it was based on that it must be a technique that can be applied considering availability of resources, knowledge, time and money. Considering many of the laser techniques they usually require specialists skills, time for the set up and is probably quite expensive. The Aspirating probe technique was refused based on the same argument. The Schlieren technique is contrary a simple method and could be a good complement to analog technique. But it was also rejected due to lack of time.

Finally the cold wire- and hot wire technique were chosen to measure the flow since the techniques and knowledge required were available at the department.

Chapter 4

Hot/Resistance wire theory

Hot-wire probe is in first hand a measure tool for turbulence. Its ability of having high sensitivity to fast flow changes with high time response is advantageous. There are mainly two different types of anemometers the constant temperature anemometer (CTA) and the constant current anemometer (CCA). Nowadays the CTA is almost always used as the velocity sensor because it's fast response due to a feed back amplifier. Both the techniques are based on heat transfer to the wires which get a resistance change when it is affected by the flow when it has another temperature then the wire. The temperature that it experienced is the total temperature, Christiansen (1961).

4.1 The CTA technique

A schematic picture of the principle of a constant temperature circuit incorporating a Wheatstone bridge, which the hot-wire is placed in, and a feedback amplifier is illustrated in figure 4.1. The Wheatstone bridge consists of four arms of whom two have fixed resistances and one has adjustable resistance and one is the hot-wire probe. Before operation the adjustable resistance is set to a value which decides the overheat temperature. When the flow changes, the resistance of the hot-wire changes and thus an unbalance in voltage occurs. The feedback amplifier reads this voltage change and convert it to an output-current which is inversely proportional to the hot-wire resistance change. The feedback amplifier reacts rapidly and stops giving current when the circuit is in balance again, Lomas (1986) & Bruun (1995). The higher amplification the shorter time it takes to get the circuit in balance.

4.2 The CCA technique

The current is held constant and the overheat ratio is adjusted in a specific flow case by adjusting a resistance placed parallel to the wire. In operation mode a change in the flow condition will result in a temperature change in the wire and therefore a change in the resistance which gives a change in the voltage output. Since there is no feedback amplifying it will have low frequency response, however the response can be adjusted by using frequency compensation (which was not implemented in the CCA used in this ex-

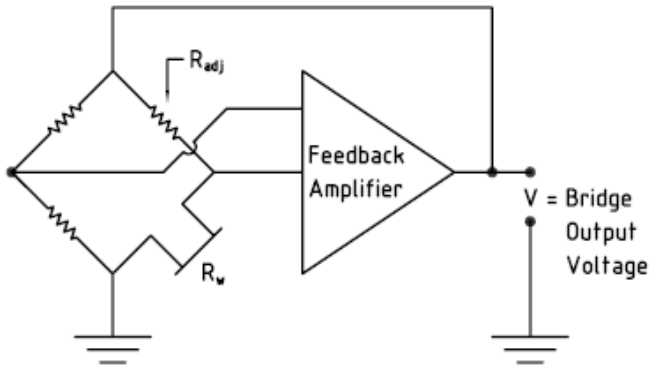


Figure 4.1: Schematic picture of the CTA circuit

periment), Lomas (1986).

The resistance wire:
When running the CCA at a very low current, the electrical heating of the wire will be negligible and it is possible to say that the wire has the same temperature as the ambient flow. That is why it is used to be called "cold wire". Thus, a speed change in the flow will not, due to convection, affect the heat balance of the wire. The only thing that can affect the heat balance is then a change in the flow temperature.

4.3 Heat transfer of wires

By studying the convective heat transfer of a finite cylinder following equation can be obtained:

$$k_w A_w \frac{d^2 T_w}{dx^2} + \frac{I^2 \chi}{A_w} - \pi d h (T_w - T_a) - \rho_w c_w A_w \frac{dT_w}{dt} = 0 \tag{4.1}$$

Where d is the wire diameter, h is the heat transfer coefficient, T_w is the wire temperature, T_a is the ambient fluid temperature, k_w is the thermal conductivity of the wire, A_w is the cross section area of the wire, ρ_w is the density of the wire, c_w is the specific heat of the wire per unit mass and χ_w is the electrical resistivity of the wire.

The conductive heat transfer rate doesn't decrease for a longer wire, but relative to forced convection it does, which is wanted. So for a wire assumed to be infinite long the conductive heat transfer can be neglected (the first term in equ. 4.1). Assuming steady state the time dependent term also vanishes. That together with the following definition of wire resistance $R = \chi / A_w$ equation 4.1 can be written as

$$\frac{E^2 R_w}{(R_s + R_w)^2} = (A + BU^{0.5})(T_w - T_a) \tag{4.2}$$

using King's well known law. Where R_s is the bridge resistance in series with the wire resistance, R_w. When including the resistances and temperatures in the coefficients equation 4.2 will have the final appearance.

$$E^2 = A + BU^{0.5} \tag{4.3}$$

4.4 Frequency response of wires

If the l/d ratio is large enough so that end losses to the prongs can be ignored, and that the temperature along the wire is uniform, the corresponding unsteady heat balance for the total wire element can be written as, Bruun (1995).

$$I^2 = (R_w - R_a)(A + BU^n) + \rho_w c_w A_w l \frac{dT_w}{dt} \tag{4.4}$$

By expressing T_w in terms of R_w (using the relation $R_w = R_0[1 + \alpha_0(T_w - T_0)]$) this yields

$$I^2 R_w = (R_w - R_a)(A + BU^n) + \frac{C_w}{\alpha_0 R_0} \frac{dR_w}{dt} \tag{4.5}$$

where $C_w = \rho_w c_w (\pi/4) d^2 l$ is the thermal capacity of the wire element. It can then further be rewritten as:

$$\frac{C_w}{\alpha_0 R_0 (A + BU^n - I^2)} \frac{dR_w}{dt} + R_w = \frac{(A + BU^n)}{(A + BU^n - I^2)} \tag{4.6}$$

From this equation the time constant is defined as:

$$M = \frac{C_w}{\alpha_0 R_0 (A + BU^n - I^2)} \tag{4.7}$$

This equation can be applied to both as a hot wire running with high overheat ratio and as a resistance wire. We can see that M is dependent of U. That equation can also be expressed in terms of Nusselt number:

$$M = \frac{\rho_w c_w d^2}{4kNu}\frac{R_w}{R_a} \cong \frac{\rho_w c_w d^2}{4kNu} \tag{4.8}$$

using the commonly used equation for Nusselt number, assuming constant Prandtl number $Nu = \frac{E_w^2}{R_w \pi l k (T_w - T_a)}$ and ignoring the current term. Equation 4.6 can also be expressed in the form:

$$M\frac{dR_w}{dt} + R_w = R_a \frac{\pi l k Nu}{\pi l k Nu - I^2 \alpha_0 R_0} \tag{4.9}$$

As named before the time response from the temperature probe is of great importance since the temperature is supposed to change rapidly. Compared to the hot-wire probe, which runs in constant temperature mode, the cold-wire has much longer time response. The hot wire runs in constant temperature mode which gives a large decrease in the effect of thermal inertia, since the circuit behind has an amplified feedback which gives very fast response when it feels an unbalance in the Wheatstone bridge. Dantec dynamics (www.dantecdynamics.com) uses the following relation between the time constant of the system for CTA and CCA, $\tau_{CTA} = \frac{\tau_{CCA}}{2aSR_w}$. Where a is the overheat ratio, S is the amplifier gain and R_w is the wire hot resistance.

John C. LaRue & Gibson (1975) has described how to compute the frequency response and the time constant.

A solution to equation 4.9 can be found by solving for constant M:

Thus M, can now be identified as the time constant. With the following definition of the 3 dB frequency

$$S \equiv -3 = 10log_{10}\frac{\overline{[T_w(f_{3dB}) - \overline{T}_w]^2}}{\overline{[T_w(f_0) - \overline{T}_w]}} \tag{4.10}$$

where f_0 is some low frequency where the imposed temperature variance is equal to the wire temperature variance, it can be shown from **??** that the 3dB frequency can be expressed as:

$$f_{3dB} = \frac{1}{2\pi M} \tag{4.11}$$

A reduction of the amplitude with 3dB is the same as a reduction of 29.28 %. Thus, to find the frequency response equation 4.8 has to be solved. The Nusselt number that was used was defined by (Collis and Williams) and yields for Reynolds number, Rd, less then 0.5.

$$Nu = (1.18 + 2Kn - 1.10dlog_{10}R_d)^{-1} \tag{4.12}$$

Where $Kn \equiv \lambda/d$, $R_d \equiv Ud/\nu$,λ is the mean free path of an air molecule at the ambient temperature and pressure, U is the fluid velocity and is the kinematic viscosity evaluated at the film temperature. Finally the expression for the time constant using equation 4.8 is (The current term is neglected):

$$M = (\rho_w c_w/4k)(2\lambda d + 1.18d^2 - 1.10d^2 log_{10}(Ud/\nu_f)) \tag{4.13}$$

In the graph below the 3dB frequency response is shown for a tungsten and platinum wire of 2.5 μm in diameter for three different nusselt numbers and for varying velocity, see Figure 4.2. Apart from the nusselt definition above, Kramer's ($Nu = 0.42Pr^{0.2} + 0.57Pr^{0.33}Re^{0.5}$) and Hilbert's ($Nu = 0.989Re^{0.33}Pr^{1/3}$ for $0.4 < Re < 4$, Incropera (1981)) definitions were also compared.

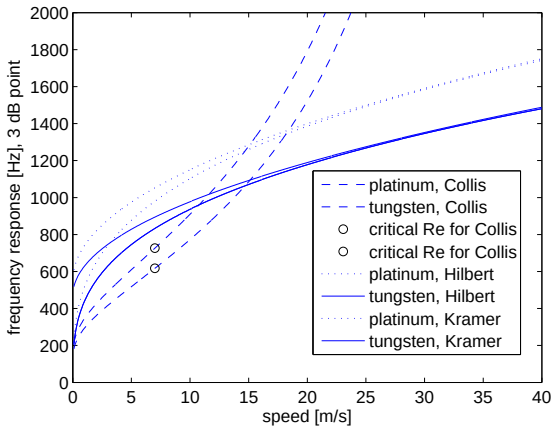


Figure 4.2: Wire frequency response, 2.5 μm wire, ambient temperature 200 C

The higher frequency response curve is when the wire is made of platinum. The importance of thin wires for high frequency response is shown in next graph, figure 4.3, where the wire diameter has been varied from 2 to 6 μm for tungsten wire using the Nusselt's number defined by Hilbert. Looking at the 5 μm curve you will get a feeling of how fast the resistance wire in the experiment will react.

4.5 Choice of wire material

For the first experiments tungsten hot wires were used and they resulted in the decision to change wire material since temperature they could be run in were too low.

To change wire material some aspects must be considered. At first the material should be able to stand at least 700 $^\circ C$. It should not loose in tensile strength and the possible

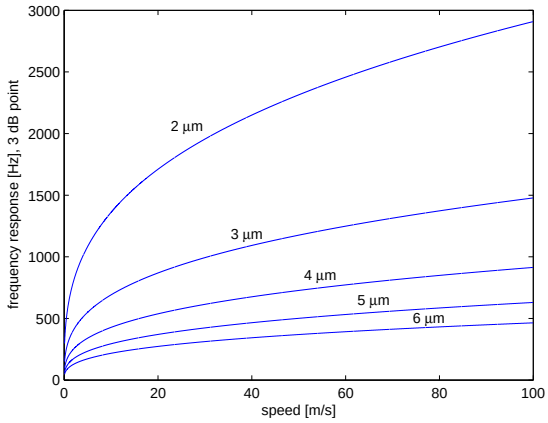


Figure 4.3: Wire frequency response, wire diameter from 2 - 6 μm

increase in wire diameter should preferably not result in a too high response increase compare to the tungsten wire. And at the end the resistance of the wire plus probe and circuit in running mode should not exceed the resistance range of the anemometry.

Following wires were compared to tungsten 5 μm in diameter and 3 mm in length:

1. Pure platinum, 25 μm, 3 mm.
2. Platinum rhodium alloy 90% / 10%, 10 μm, 3 mm.
3. Platinum iridium alloy 80% / 20%, 10 μm, 3 mm.

Following wire material analysis are based on chapter two in Bruun (1995).

A wire element at uniform temperature is given by: $R_{20} = \chi l/A_w$ where χ is the resistivity at 20 $°C$, l the length and A_w wire cross section area. Implementing this resistance in following equation $R_w = R_{20}[1 + \alpha_{20}(T_w - T_{20})]$ the resistance at the running temperature will be obtained. That was done for the three cases and compared to the tungsten wire. The three alternative materials were supposed to be heated to 700 $°C$ Following results were obtained:

Wire	quota ($R_{w,x}/R_{w,tung}$)
1	0.17
2	1.20
3	1.53

It can be seen that the pure platinum wire will get very low wire resistance compared to the tungsten wire because its thickness. While the other two platinum wires got a little bit higher resistance, but still not too high, since the resistivity of the material is higher. Fortunately they have a very low temperature coefficient of resistance, α, so the resistance does not increase too much when it gets heated.

Considering the end losses they should not be to high due to the reduction of time response and invalidity of derived heat transfer laws. Therefore the quota conductive heat transfer over forced convective heat transfer should be as low as possible. In Bruun (1995) the equations for conductive end losses respective convective heat transfer are stated, see equation 4.14 and 4.15,

$$\dot{Q_{cp}} = 2k_w A_w \frac{(T_w - T_a)}{l_c} \tanh(l/2l_c) \tag{4.14}$$

$$\dot{Q_{fc}} = \pi d\iota h(T_w - T_a) \left[1 - \frac{2l_c}{l} \tanh \frac{l}{2l_c}\right] \tag{4.15}$$

where l_c is the "cold length" and is defined as $l_c = \frac{d}{2}\left(\frac{k_w}{k}\frac{R_w}{R_a}\frac{1}{Nu}\right)^{1/2}$. The quota $\frac{\dot{Q_{cp}}}{\dot{Q_{fc}}}$ is compared for the three wires to the tungsten wire, results below:

Wire	quota $\left(\frac{\dot{Q_{cp}}}{\dot{Q_{fc}}}\right)_x / \left(\frac{\dot{Q_{cp}}}{\dot{Q_{fc}}}\right)_{tung}$
1	0.12
2	0.32
3	0.31

The results shows that tungsten wire has a higher conductive - convection quota than all the other alternatives. Probably due to their small thermal conductivity coefficient since the length over diameter ratio i smaller.

The strength was computed using the tensile strength factor, γ $[N/cm^2]$, for the material to multiply by the cross section area of the wire. The results are shown below:

Wire	quota γ_x/γ_{tung}
1	3.0
2	0.96
3	2.1

It shows that all have quite high strength compared to the tungsten wire, due to that they are thicker since the tungsten material it self is stronger.

Finally the choice fall on the Platinum iridium wire since it was stronger than Platinum rhodium and still could be heated to 700 $°C$, 100 $°C$ lower than the Platinum rhodium wire. The pure platinum wire was rejected when it turned out it was not able to weld on the prongs.

All the wire material data are taken from Dantec's web site, www.dantecdynamics.com.

Chapter 5

Calibration

The temperature is supposed to vary rapidly in the flow which has to be considered when using hot wires. If you not change the settings for the CTA it will give wrong output signal. I.e. if the temperature is increasing the velocity sensor will show a lower output signal due to lower cooling effect of the wire. There are two ways to circumvent this problem:
One is to have a simultaneous changing temperature of the wire related to the temperature of the flow so the overheat ratio keeps constant which result in a cooling constant effect. Due to an absence of a re-coupled circuit of the temperature sensor and the velocity sensor and software needed for that purpose, this method was neglected. The other alternative is to keep the temperature constant and calibrate the hot wire for different temperatures of the flow. This was the chosen method, Dantec's web site www.dantecdynamics.com, Bruun (1995).

5.1 Calibration device

The hot- and cold wires were calibrated in a flow generated by a heat gun. The criterion for the choice of a flow generator was that it should be adjustable in booth velocity and temperature and that it could generate a flow with a velocity as high as possible and temperature around 600 $^{\circ}C$. The heat gun that was used was a Steinel HG 2310 LCD. It was one of few heat guns that were adjustable. It was adjustable for temperatures from around 45 $^{\circ}C$ to 550 $^{\circ}C$ and for velocities around 12 to 30 m/s. For temperature and velocity measurements a thermocouple of k-type and a common Petot-tube were used. To make the flow as uniform and turbulent poor as possible a 50 mm thick honeycomb and a 1.5 mm meshed screen were used in an extension fixed at the exit of the heat gun, see figure ... . At the end of the extension a converged nozzle, with an exit diameter of 14.5 mm, was fixed in the purpose of having a faster flow. The pictures below show the calibration set up in its running mode, figure 5.1 and 5.2. The Probes that were used were single wire probes and dual probes with one hot wire sensor and one cold wire sensor.

Following instruments were used:
A CTA for hot wires and a CCA for cold wires (only two channels), an A/D converter to

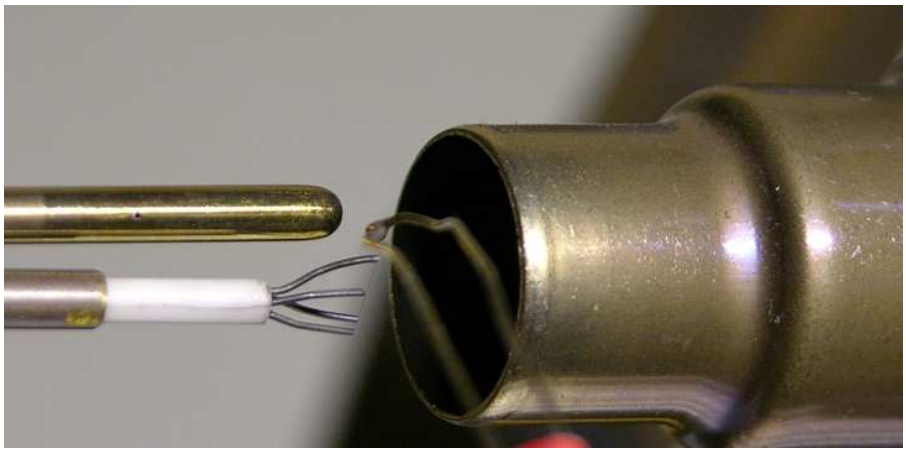


Figure 5.1: Calibration probe setup.

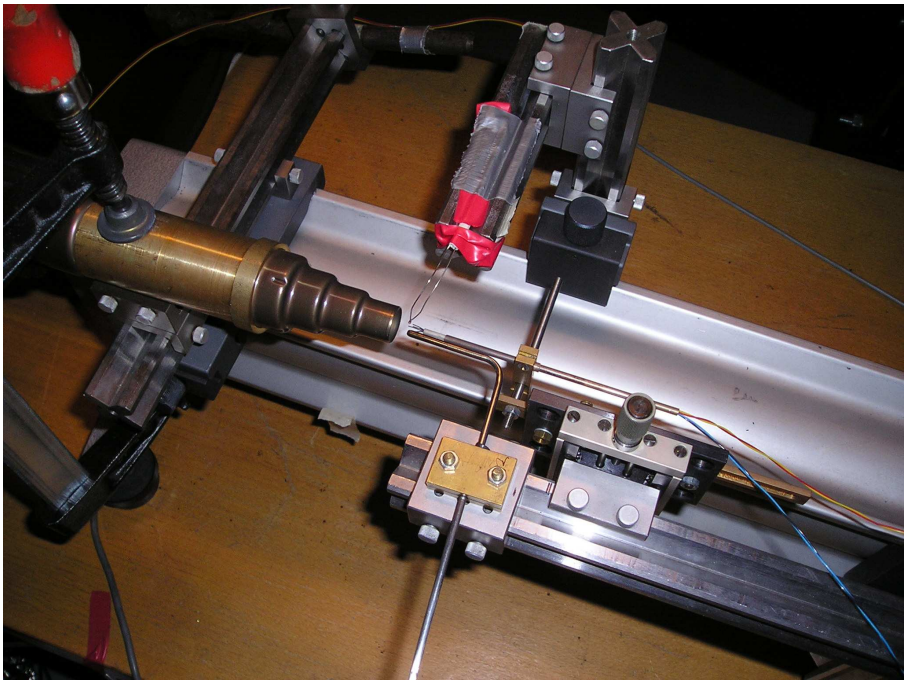


Figure 5.2: Calibration setup.

convert the analog signal from the wires to digital signal, an oscilloscope to observe the signal coming from the CTA and CCA, an anemometer to read the pressure difference from the pitot tube, a multimeter to read the voltage generated by the thermocouple, a zero degrees reservoir as a cold reference for the thermocouple so the voltage differences generated refer to Celsius degrees, a computer including the software program lab-view with a special designed program to assemble and work all digital data.

5.2 Probe manufacturing

The probes were in-house manufactured. Following components were used:
Piano wires (0.4 mm), brass pipes, ceramic tubes, glue, flux, shrink tubes, thin cables and cables contacts were the components.

The manufacturing steps:
Cut the piano wires so that they fit the chosen ceramic tube, which means that a certain length should be left over for the prongs and a certain length should be kept as soldering part to fix them on the cables. Since the brass tube is very thin the wires should have different length outside the ceramic tube. Due to the narrow tube the wires have to be covered by very thin plastic tubes so that they do not touch each other and causes a short circuit. Before the wires gets soldered they should be inclined so they form the desired prong shape, which usually depends on how long wire you want and if there is going to be more then one hot/cold wire. In this experiment there were four piano wires inclined to two parallel wire holder one three millimeter long and one four millimeter long. The piano wires are placed with glue inside the ceramic tubes. It turned out that it is important to not use too much glue since the it expands when it heats in high temperatures which causes fractures on the ceramics. The glue also loose its ability to attach. Later manufactured probes were made in a way that the ceramic tube was inserted quite long distance in the brass pipe. When the cables were going to be soldered on to the piano wires the soldering point should be as small as possible and the shrink tubes has to be short enough so that they do not overlap each other.

Wire repairing:
The wires that were used were 5 and 2.5 μm tungsten wires and 10 μm platinum alloy with 20 % iridium. The wires were fixed on the prongs by spot welding. The equipment contained a microscope, a stable probe holder, a wire holder with fine adjustment possibilities, a welding electrode holder with fine adjustment and a spot welding device. Although the equipment was quite professional it was difficult to attach the 2.5 μm tungsten wire on the prongs. It was a combination of a lack of devices and that the prongs had a very rough surface which caused the problems.

5.3 Calibration of Hot wire

CTA settings for the hot wire:

To be able to set the hot wire sensor to a certain temperature, the resistance which corresponds to that temperature must be calculated. Therefore the wire resistance in the reference temperature (room temperature) must be found. Using the temperature coefficient of resistivity the resistance in heated mode can be calculated, $\alpha_0 = 0.0036\ 1/^\circ C$ for tungsten. First the wire resistance is calculated using following formula $R = R_0[1+\alpha_0(T-T_0)]$ then the overheat ratio can be found as $a = (R - R_0)/R_0$. Knowing this the total resistance in the hot mode can be calculated:

$$R_{tot(hot)} = (1 + a)R_0 + R_c \tag{5.1}$$

Following signal analysis was made for a hot wire:
When the settings were done the signal coming out from the CTA must be observed in an oscilloscope to make sure that it is stable. It was found to be quite difficult to get a good signal for the tungsten wire. The signal oscillate a lot in ambient conditions, room temperature and no flow. As discussed before, in the case when the overheat ratio is very high the wire is sensitive to velocities. This means that it also can be interpret that the wire is very sensitive to small velocity disturbances in the environment. This statement was confirmed by looking at signal when the ambient temperature was increasing, by holding the wire in a warmer flow, then the signal got more stable. One way to handle this problem is to reduce the gain. High gain amplifies the disturbances so the signal starts to self oscillate, although the gain was reduce to the minimum value still there were sometimes oscillations. The solution to that was to heat the wire in a hot flow around 300 $^{\circ}C$ or/and have the probe connected to the CTA set to held the wire to a temperature around 300 $^{\circ}C$. The signal could also be checked by implement a square wave and observe how the system responds to it. If the signal goes back to its original amplitude without a tail of oscillations then the signal is good.It turned out that there were no problems with the platinum iridium wire which has much lower α_0 making the wire less sensitive to temperature changes. With implementation of the square wave it is also possible to get the frequency response of the system.

Hot wire data assembling:
The assembling procedure was performed by a lab view program. The disadvantage was that the program did not record the mean value of the dynamic pressure values from the pitot tube under the record time; instead it took only one sample after an unknown time. Since the flow had a significant low frequency unsteadiness the pressure values will not always correspond to the voltage values register from the hot wire as a mean value over the record time. The mean value of voltages would also differ a lot from its true mean if it is not based on a long record time.

The lab view program is built in a way that you set the samplings rate and the number of samples. The decision of the setting values is based on following:
1) To get a better estimation of the pressure values, the record time could be divided into many parts to obtain a kind of poor mean value of the pressure. In this case it was divided into three parts.
2) The record time desired to get a good mean value of the voltages.
3) The time available for this calibration.

Finally the settings were set to 2000 Hz samplings rate and 30,000 samples that is a record time of 15 seconds, this record was done three times for each flow rate. In fact the voltage values didn't change very much for the three records, although the record series only contained by few number of low frequently peaks. The number of peaks varied between 5 and 1 depending on the settings of the heat gun. The three measurements made an improvement of the pressure registration and a group of points represented every flow

change and thus made the curve fitting more realistic.

For the first case when tungsten was used as hot wire material the calibration was divided into six temperature steps between 133 and 332 $°C$. In case two temperature division went from 85 to 335 $°C$ and in the third case from 89 to 341 $°C$. Since tungsten still was used as material for the resistance wire in case two and three, the temperature range could not be increased even though the platinum iridium wire could withstand higher temperatures. The flow rate steps were divided into ten and went from lowest to highest possible rate from the heat gun.

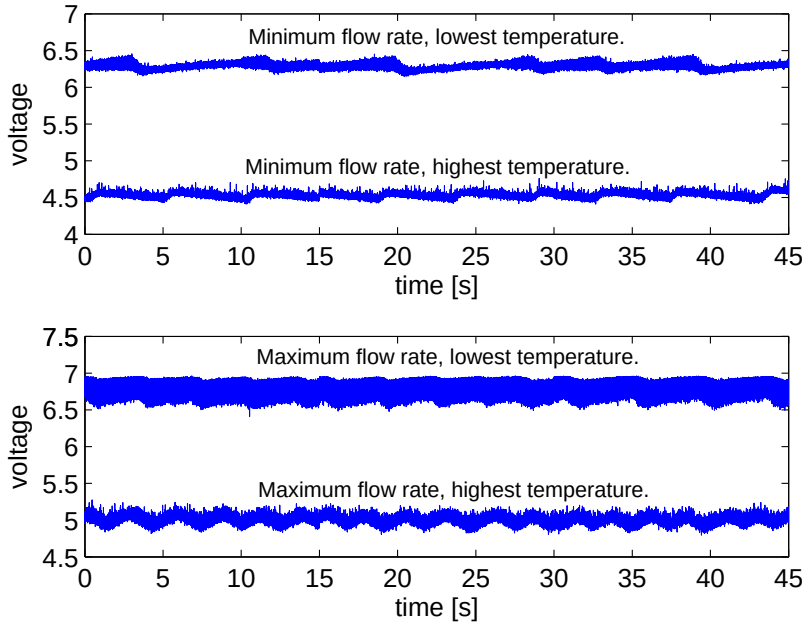


Figure 5.3: Hot wire signals from HW4, case 3, for minimum and maximum flow rate and temperature

1. The simplest method of describing the relation is to say that the heat transfer is proportional to the product of the temperature difference $T_w - T_a$ and a function of the velocity. T_w is the wire temperature and Ta is the ambient temperature. Following expression shows the relation: $E^2 = f(U) * (T_w - T_a)$.

2. The convective heat transfer is expressed in a non-dimensional form involving a relationship between the Nusselt number, Reynolds number and Prandtl number.

3. Direct calibration of the variation in the voltage, E, with the velocity, U, and the fluid temperature, T_a, for a given hot-resistance setting, R_w.

The relation between voltage and velocity was chosen between a power law equation, Kings law $E^2 = A + BU^n$, and polynomial equation of forth order or less, $U = A + BE + CE^2 + DE^3$. The choice fall on the power law, which is more accurate in the

interval between 5 and 50 m/s Bruun (1995) and which is more stable outside the interval.

The data that was collected in this calibration was analyzed in a direct method, trying to get a unique, empirical found relation how these certain hot wires react in a flow when temperature and velocity varies. As said before a power law, namely the King's Law, was applied to fit the data for varying speed since it is more stable outside the calibration range and the power, n, in this equation was chosen to 0.5, this implies that the wire is assumed to be infinite long, Bruun (1995). The reason why this coefficient was fixed was also that it was impossible to get nice parallel curves outside the calibration range if it wasn't. Since the data points were not idealized collected and therefore gave the risk for a several different curves to be fitted to them. The coefficients A and B in the different calibrating curves were analyzed to see how they varied. They seemed to have a linear relation with temperature, thus they were replaced by a first order polynomial equation dependent on temperature, see figure 5.5. Finally the calibrating function had the form:

$$E^2 = a_1 + a_2(T_w - T_f) + (b_1 + b_2(T_w - T_f))U^{0.5} \tag{5.2}$$

Where T_w is the wire temperature, T_f is the temperature of the flow, U is the speed and E is the voltage. A similar calibration curve have been found by a lot of other people. In figure 5.4 one example of a hot wire calibration function is shown for the same temperatures as the data points were collected for. Obviously the function works very well in the calibration temperature region, which can be seen when the calibration observation fits with the curves generated from the function. It turned out that the calibration function didn't work well if the temperature went to much above the highest calibration temperature.

5.4 Calibration of Resistance wire

The resistance wire was fixed parallel to the hot wire on the same probe but with a short distance further downstream. Two different current strengths were used, 0.1 mA and 0.2 mA, the reason for that was to see if the lower voltage output observed for higher velocities depended on the current strength. It turned out that it was not the reason and probably it was the heat gun itself that couldn't keep the temperature constant. The anemometer had the advantages of having a back off function which means that the output voltage in reference mode is set to zero, that make it possible to avoid the signal to reach the out put voltage roof due to the amplifying being implemented. The resistance wire generated voltages were correlated to the temperature obtained from the thermocouple. Here the low frequency unsteadiness of the heat gun flow resulted in difficulties to observe correct mean temperature since it was recorded manually by watching the voltmeter. When the resistance wire sat on the same probe as the hot wire, the voltage was registered for the lowest speed since it decreased for increasing speed. The voltage- temperature relation were fitted to a linear curve having the appearance:

$$T = T_a + cE \tag{5.3}$$

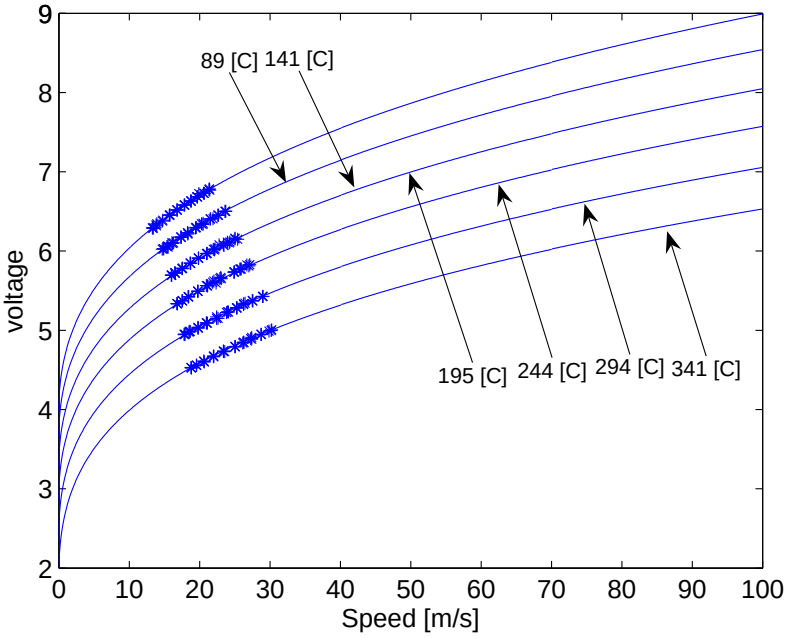


Figure 5.4: Calibration curves for HW4, gas generator 7.

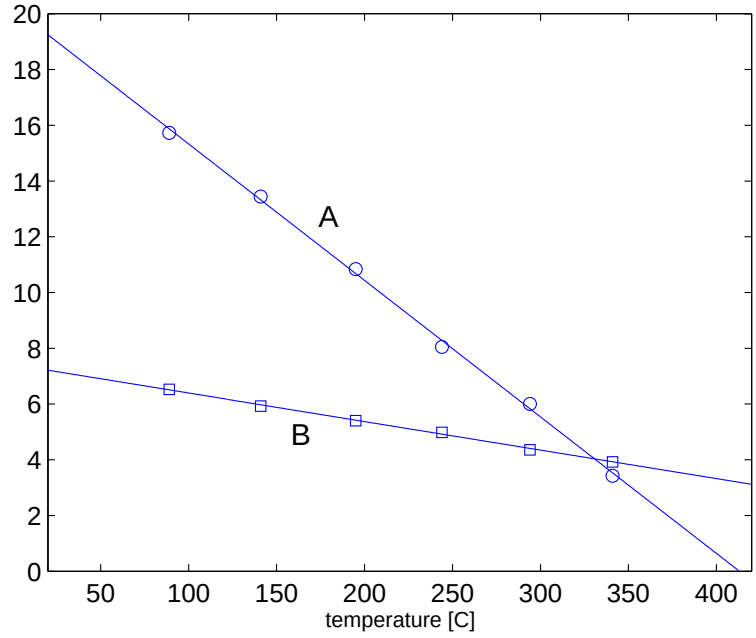


Figure 5.5: The coefficients A and B varying with temperature

Where T_a is the ambient temperature and c is the calibration coefficient and E is the voltage.

An example of how a resistance wire calibration look like is shown in figure 5.4.

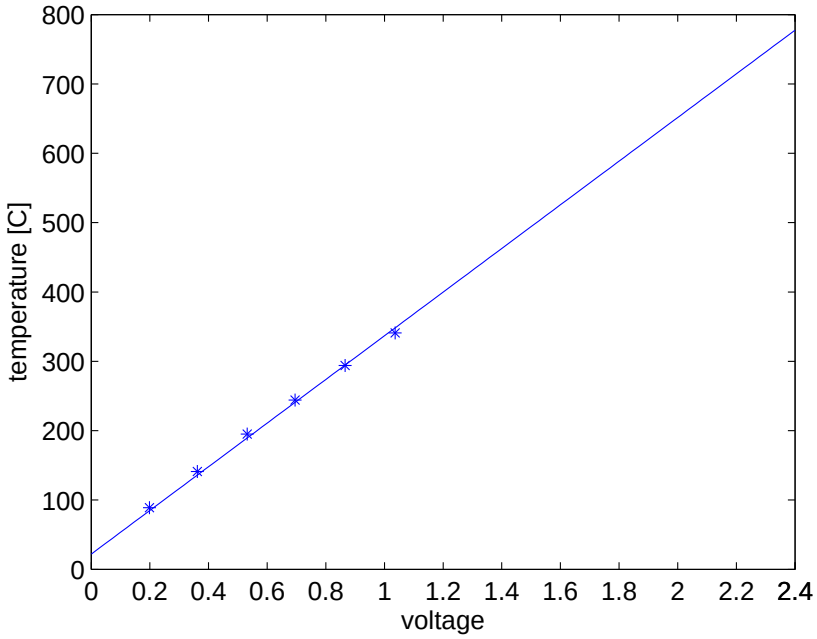


Figure 5.6: Resistance wire calibration curve

Chapter 6

Experiment procedure

The measurements were made in a kind of cylindrical extension, see figure 6.1, between the gas generator and the airbag in the purpose to have a place to have the probes. A drawing of the extension is shown in figure 6.2.

The time it takes for a boundary layer to grow is slow enough to assume that the velocity and temperature profile is constant through the cylinder. This statement can be defended by the equation below, equation 6.1, (Panton).

$$\delta = 3.6\sqrt{\nu t} \tag{6.1}$$

Where δ is the boundary layer thickness, ν the kinematic viscosity and t is the time. Due to the very quick event taking place no boundary is assumed to be created Instead a flat velocity and temperature profile is assumed to propagate upward behind a shock wave. To confirm that, the hot wires in the first experiment were placed with different radial position. In the experiment after that the probes were placed in the same radial position and height to see if the results from the probes are the same. In the last experiment the wires were placed in the radial center but at different heights to see how fast information is propagating in the extension cylinder and to analyze possible shock- and expansion waves. Twice dual hot wire was used to try to get the temperature this way. In the last five airbags inflations pressure sensors were placed in the extension cylinder.

The measurements were made in three sets, with different measurement setups and different kind of probes and locations in the cylinder. Ten gas generators were used, one air bag inflation will be considered as one experiment. But all of the gas generator releases will not be presented in the results since problems occurred for some experiments, where wire breaks was the most common reason why the experiment had to be rejected. Table 6 shows the experiment configurations.

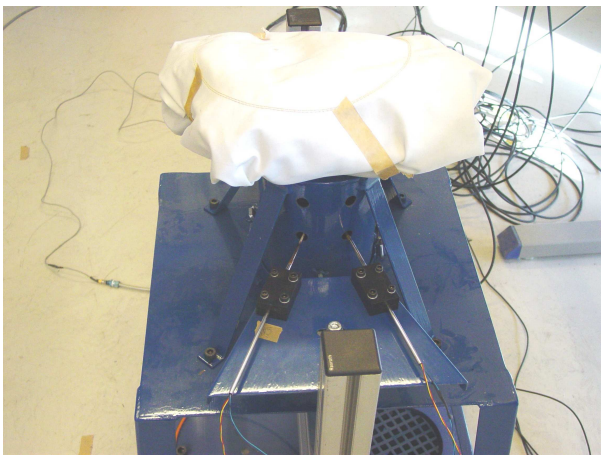


Figure 6.1: Experimental set up

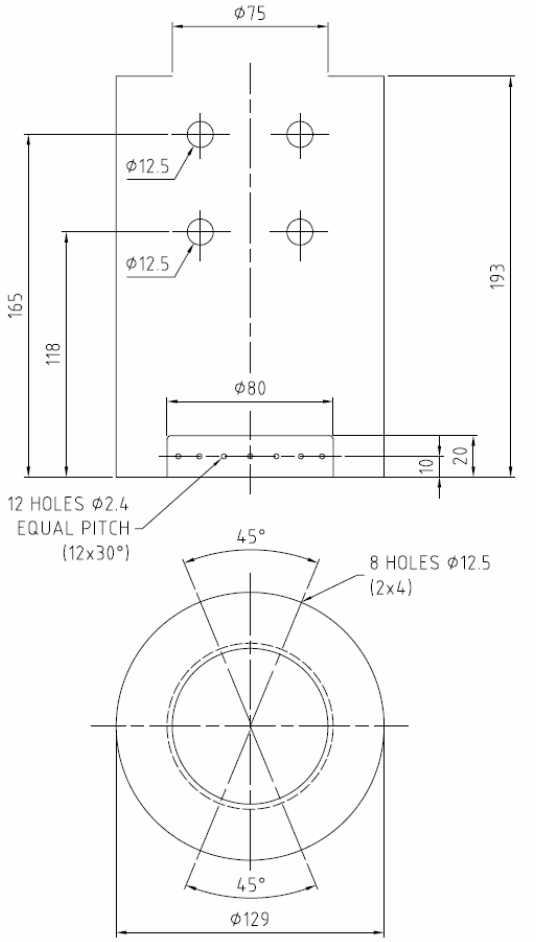


Figure 6.2: Design of the gas generator extension

Case	Experiment (Gas generator)	Comments
1	1	
	2	One dual HW/CW probe, 2.5 μm tungsten wire as cold wire and 5 μm tungsten wire as hot wire heated to 400 $^{\circ}C$. And one single hot wire. All located at 165 mm but the dual probe was located at 37 mm inside the cylinder while the single hot wire was located 51 mm inside.
2	3	Two dual HW/CW probes, 5 μm tungsten wire as cold wire and 10 μm platinum alloy with 20 % iridium as hot wire placed at the hight 118 mm. HWCW3 was placed two thirds inside the cylinder and HWCW2 one third, both at height 118 mm.
	4	Two dual HW/CW probes, HWCW4 and HWCW6, 5 μm tungsten wire as cold wire and 10 μm platinum alloy with 20 % iridium as hot wire placed at hight 118 mm and both with the half radius inside the cylinder.
	5	One dual hot wire running in 700 respectively 600 $^{\circ}C$, one single cold wire, CW5, and one further cold wire from previous experiment, CW6. All of them placed in half the radius at hight 118 mm.
3	6	Two dual HW/CW probes, 5 μm tungsten wire as cold wire and 10 μm platinum alloy with 20 % iridium as hot wire. Both are placed in the center with the distance ca 47 mm from each other, HWCW1 at hight 118 mm and HWCW2 at hight 165 mm.
	7	The same probe composition as above but with two different probes, HWCW3 at hight 118 mm and HWCW4 at hight 165 mm.
	8	Two single cold wires placed in the center with the distance ca 47 mm from each other, singleCW1 at hight 118 mm and singleCW2 at 165 mm. And a double hot wire probe, a platinum alloy with 10 % rhodium at hight 118 mm.
	9	Using the same wires and the same probe composition as in experiment 1
	10	Using the same wires and the same probe composition as in experiment 1

Table 6.1: Experimental configurations

Chapter 7

Results and analysis

The results consist of signal analysis from resistance wires, hot wires and pressure sensors. The signal from the resistance wire was converted to temperature (total temperature) and as long as the calibration is trustable the result could be used. The temperature measurements will also be used to analyze property changes across the shock wave. The signal from the hot wire will mainly be used as help to analyze the events occurring, by looking at the time when events appears. Since there were problems to convert the hot wire to fully velocity time series.

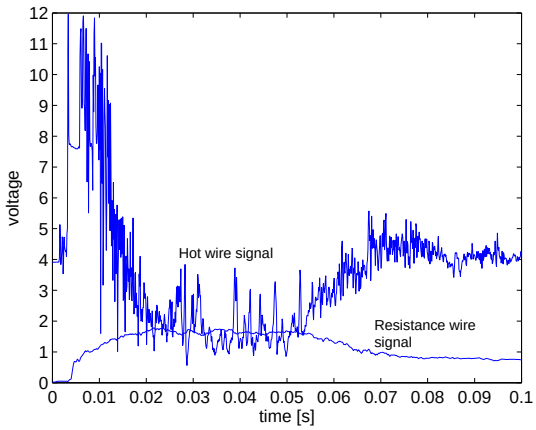


Figure 7.1: Raw data plotted from HW1 and CW1 for gas generator 10.

In the third case a pressure sensor was placed in the bottom of the extension, the result from this will show the pressure changes, but it will also be used together with the temperature to compute a density time series. In the same case a movie also was recorded it showed that the air bag was fully inflated in 35 - 45 ms. An example is presented of how the raw data looked like from the hot- and resistance wire, figure 7.1. It shows very clear that the hot wire voltage output decreases when the signal from the resistance wire increases which is a very expected result.
The noise that is registered in the beginning of the hot wire signal is probably electrical noise starting when the gas generator gets its electrical signal which starts the combustion process.

7.1 Temperature measurements

Temperature measurements were made before with so called cold wires. Some of them broke and some of them were used for more than one measurement. The wires that were

used for gas generator 6 were used twice more, in 9 and 10. Resistance change in the wire shouldn't affect the result since back off adjustments were used. The temperature measurements are shown for gas generator 2 to 5 in figure 7.2 and for gas generator 6 to 10 in figure 7.3. It should be mentioned that it is not the static but the stagnation temperature that is measured, Christiansen (1961). But since the temperatures are so high the dynamic part of the total temperature will be very small. The measurements where the wires were broken are also shown with a clear change in signal level when it rapidly raises to the top of the picture.

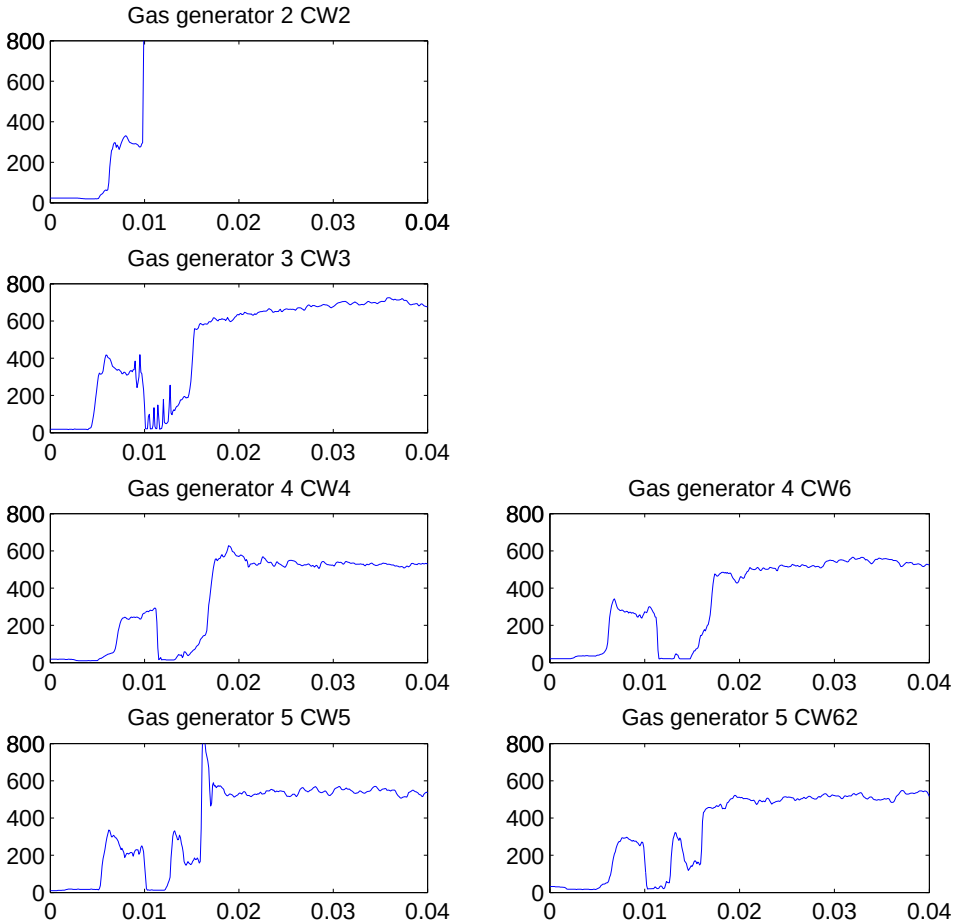


Figure 7.2: Stationary temperature profiles [°C] plotted against time [s] for case 1 & 2.

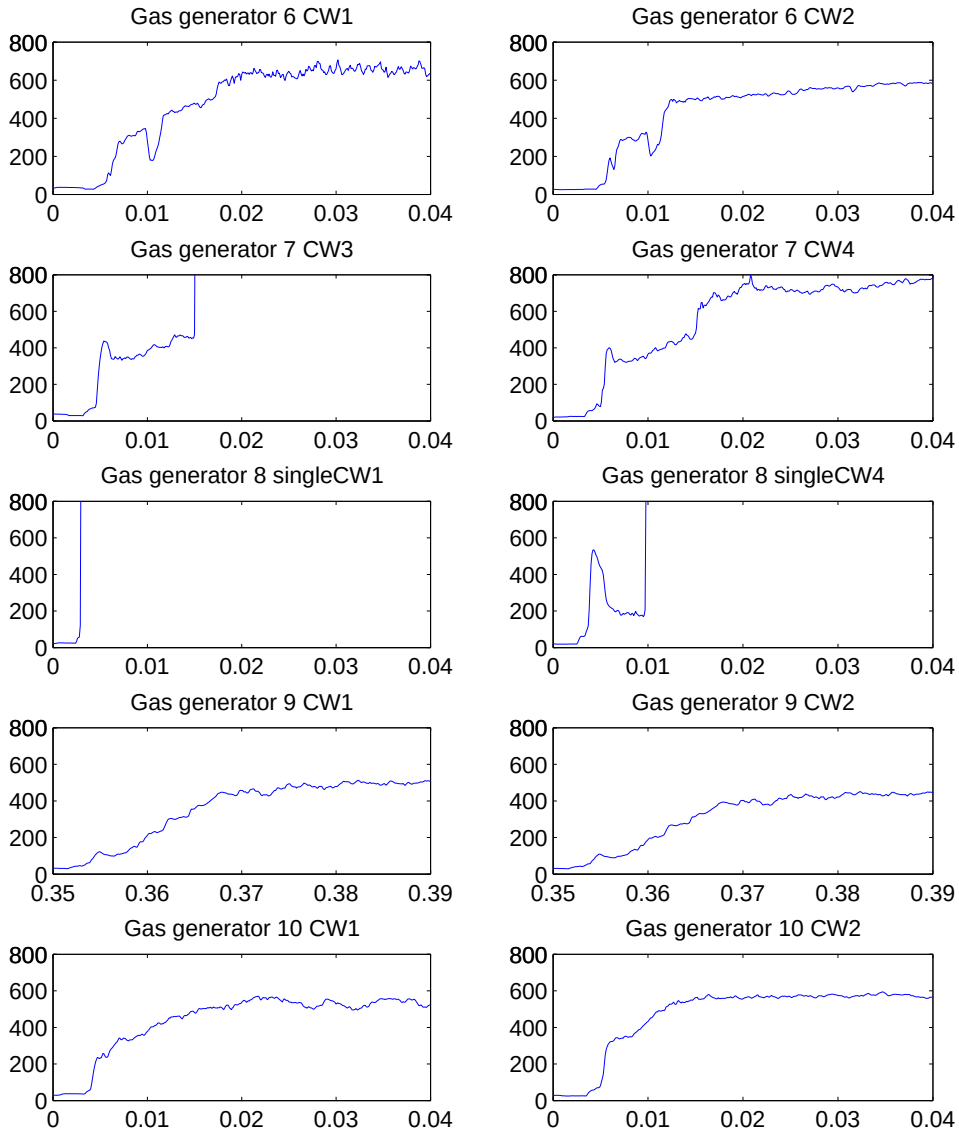


Figure 7.3: Stationary temperature profiles [°C] plotted against time [s] for case 3.

7.2 Time response

For the platinum iridium alloy hot wire a higher gain could be used without getting the signal to oscillate compared to the tungsten wire. That is probably because of the lower temperature resistivity and thickness of the wire compared to the tungsten wire. The benefit to have a high gain is that the time response becomes quicker. It was set to 11912 for the platinum iridium hot wire and for the tungsten hot wire it was set to 3470.

In a square wave test in ambient condition with no flow the 3dB frequency response was computed to be ca 6.1 kHz for the platinum iridium wire and 15.3 kHz for the tungsten wire. Of course the frequency response increases in a flow since it depends on the speed, so the value above can be considered as the lowest possible 3dB frequency in the experiment.

To estimate the resistance wire frequency response the temperature increase due to the shockwave is used, since this step change occur very fast due to the high speed of the wave. The 3dB point frequency was found by the well known formula for a step change, see equation 7.1.

$$f_{c(3dB)} = \frac{0.35}{t_{raise}} \tag{7.1}$$

Where t_{raise} is defined as 90% of the time it takes for the signal to reach its final value after a step change.

In the gas generator 6 experiment the resistance wire CW2 showed a very clear response to the shock, see figure 7.4. Using equation 7.1 the 3dB frequency become 556 Hz, $f_{c(3dB)} = 0.35/(0.9 \cdot 0.0007) = 556Hz$.

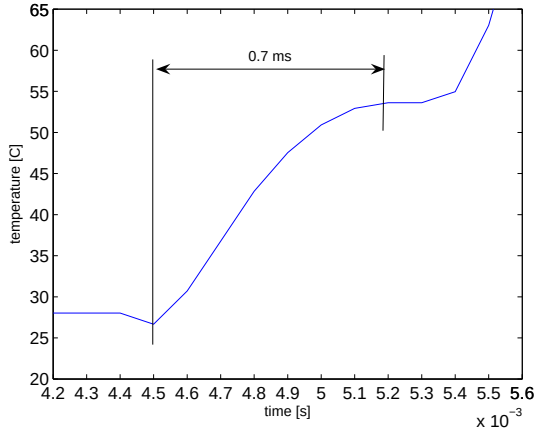


Figure 7.4: Temperature step for CW2, gas generator 6.

7.3 Comparison with compressible flow theory

As can be seen from the hot wire signals, it obviously occurs a shockwave. Then it make sense to use the theory about property changes across a shock wave which was discussed in chapter 2. From the total temperature time series measured by the resistance wire it should be possible to observe the phase changes, first an increase in temperature after the shock wave passes and after that a further increase occurs when the hot gas passes. In the tables below the property changes are shown for some gas generators and probes.

	CW1 & CW2
u_p	69 m/s
W	391 m/s
P_2/P_1	1.32
ρ_2/ρ_1	1.22
$\dot{m}$	1.33 $\frac{kg}{s}$

Table 7.1: Results from gas generator 6

	CW4
u_p	80.7 m/s
W	398 m/s
P_2/P_1	1.38
ρ_2/ρ_1	1.26
$\dot{m}$	1.62 $\frac{kg}{s}$

Table 7.2: Results from gas generator 7.

	CW2
u_p	99 m/s
W	408 m/s
P_2/P_1	1.48
ρ_2/ρ_1	1.32
$\dot{m}$	2.1$\frac{kg}{s}$

Table 7.3: Results from gas generator 2

	singleCW2
u_p	108 m/s
W	413 m/s
P_2/P_1	1.53
ρ_2/ρ_1	1.35
$\dot{m}$	2.31$\frac{kg}{s}$

Table 7.4: Results from gas generator 8

Since Hugoniot equations only are valid for static properties the stationary temperature must be converted to static temperature and that can be done if the velocity is known referring to the well known relation for stationary temperature, equation 7.2.

$$T_0 = T + \frac{u_p^2}{2C_p} \tag{7.2}$$

This equation closes the equation system and makes the calculations to an iterative procedure. Thus, the temperature difference must first be found. The temperature after the shock is taken when the temperature reaches a some what constant value, if there is no plateau it is taken in the transition to the gas, since it could take time for the resistance wire to respond. But looking at plots the question is where the transition to gas occurs. To know this another iterative process must be applied. There are some shapes in the temperature series that could be the air to gas step change. But if the time it should take for the shockwave to reach the probes is studying, it can be observed. Using equation 2.4, 7.2 and 2.7 the induced speed of the air/gas behind the shock wave can be found. And from equation 2.6 the speed of the shock wave is determined. Knowing the speed of the wave and gas, and knowing the distance to sensor from the gas source it can be evaluated

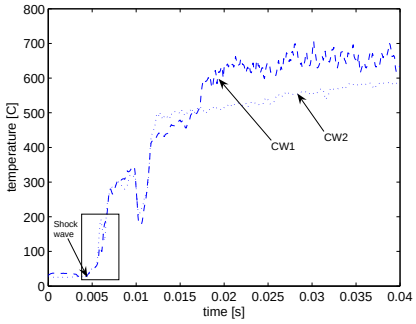


Figure 7.5: Temperature profiles from gas generator 6 for CW1 & CW2, temperature increase induced behind the shock wave is found the square.

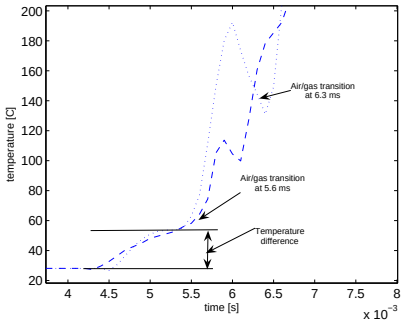


Figure 7.6: Enlarging the square above the temperature difference, which the shock wave calculations are based on, can be seen, Gas generator 6.

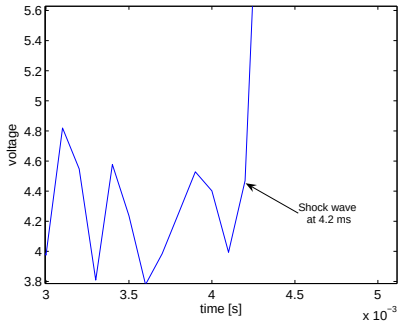


Figure 7.7: The time when the shock wave occurs for gas generator 6

if the time until the air/gas transition occurs is reasonable.

The data shown in the table 7.1 - 7.4 were obtained from the temperature differences. Knowing the ambient conditions, static density pressure and temperature, ρ_2, P_2 and T_2 can be determined after the shock. Therefore the mass flow after the shock could be computed, see table 7.1, using equation $\dot{m} = \rho_2 u_p A = (P_2/(T_2 R))\, u_p A$. Where A is the area of the cross section of the cylinder.

The decision of the location of the transition region is based on that the time between the shock wave and the transition from air to gas is observed. The distance, l_{p1}, from the bottom of the cylinder to the first probe is 118 mm and assuming the gas and the shock wave having their origin at the bottom the time between the shock wave and the gas, t_{p1}, is:

$$t_{p1} = l_{p1}/u_p - l_{p1}/W \tag{7.3}$$

For example in figure 7.7 it can be seen that the the shock wave occurs at 4.2 ms and in figure 7.6 it can be seen that the transition occurs at some where around 5.5 ms. Using equation 7.3 and the values for u_p and W from table 7.1, $t_{p1} = 1.36$ ms. That gives a transition location at 5.56 ms which shows that the transition occurs around that time and that the temperature after the shock is quite reasonable. The dotted line in figure

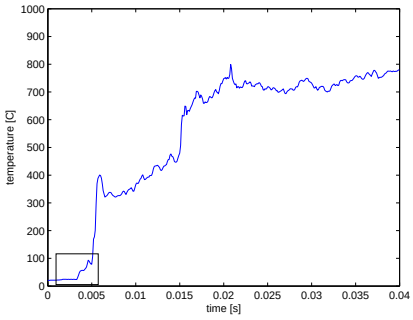


Figure 7.8: Temperature time series for gas generator 7 CW4, temperature increase induced behind the shock wave is found in the square.

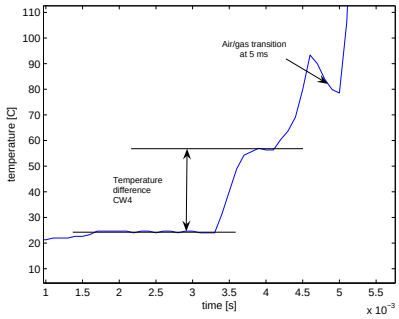


Figure 7.9: Enlarging the square above the temperature difference, which the shock wave calculations are based on, can be seen, gas generator 7.

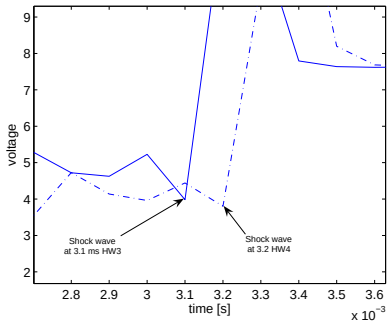


Figure 7.10: The time when the shock wave occurs for gas generator 7.

7.6 and 7.5, CW2, shows a little bit too low temperature concerning the gas transition which appear too late.

Doing the same analysis on gas generator 7 following results can be determined, see table 7.2, based on figures 7.8 - 7.10. Also here it is possible to see that the transition to gas does not appear at same place as it is supposed to do. Probably it depends on where the shock wave establishes.

Finally two more gas generator result is presented, gas generator 2, case one. The temperature ratio across the shock wave gave following result, see table 7.3 and figure 7.11 and table 7.3 and figure 7.12. The shock strength seems to be quite high compared to the other gas generator results.

In figure 7.9 it can be seen that the temperature steps aren't so clear and they are difficult to find. That could depend on the signals which from the beginning were not stable, they contain some kind of disturbance which is periodic. Since they appear with 100 Hz frequency they probably come from the electrical net which has a supply frequency of 50 Hz. A part of this disturbance is shown to the left in figure 7.9 and a longer series is shown in figure 7.13. The difference in shock strength could also depend on the slow response time of the resistance wire so the wire has no time to feel the temperature after the shock before the gas comes. Looking at the measurements from gas generator 8, 9 and 10, it is difficult to find the the right temperature step since all of them have there

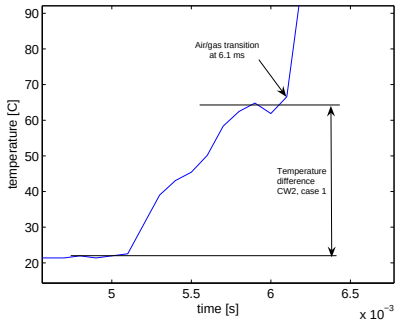


Figure 7.11: Temperature difference, which the shock wave calculations are based on for gas generator 2.

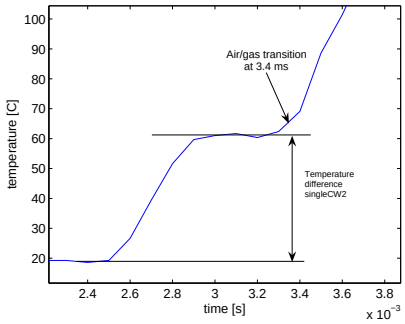


Figure 7.12: Temperature difference, which the shock wave calculations are based on for gas generator 8.

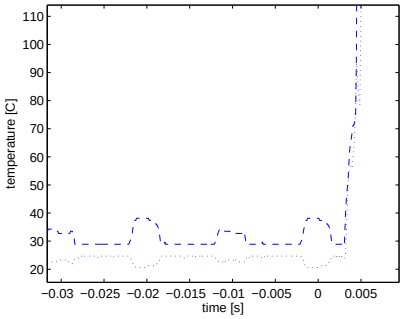


Figure 7.13: Periodic disturbances for CW3 & CW4

temperature raise at the transition region of a disturbance which makes it problematic to forecast the signals' shape if the ground level was flat.

However, the two air/gas transition points where the temperature differences were obtained from, which gave the data in table 7.2, figure 7.10 shows the time it takes for the hot wire sensors to feel the shock wave. The time difference between the two observations is 0.1 ms. Calculating the time it should take for the shock to propagate this distance using shock wave speed 394 ms and the distance between the two probes, 47 mm, it should take 0.12 ms. But since the samplings frequency only is 10,000 Hz (recording one sample every 0.1 ms) it is not possible to resolve this fast course of events.

In the third case, a pressure sensor was placed on the bottom of the cylinder. The location is not the same as the probes' but still it can be used to get some idea of the density changes in the cylinder using the temperature from the resistance wire in the equation relating pressure, density and temperature for perfect gas, $P = \rho RT$.

In figure 7.14 and 7.15 the density and pressure raises across the shock wave is shown for gas generator 6 & 7 with their correspondence to the pressure and density ratio from table 7.1 and 7.2.In figure 7.16 the density and pressure profiles are shown for gas generator 10.

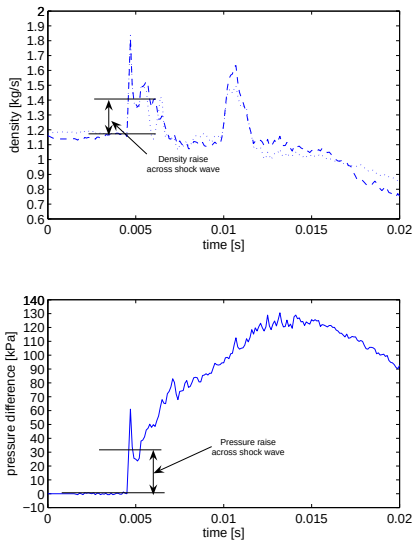


Figure 7.14: Density and pressure raise for gas generator 6

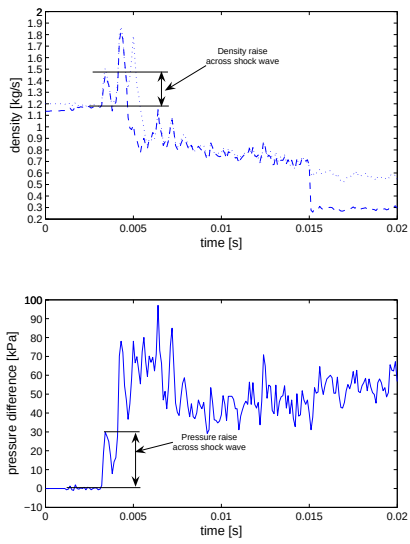


Figure 7.15: Density and pressure raise for gas generator 7

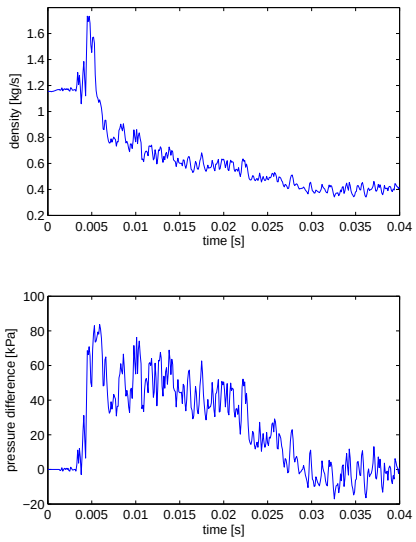


Figure 7.16: Density and pressure profiles for gas generator 10

7.4 Hot wire measurements

The hot- and resistance wire signal does not agree with each other good enough to utilize the generated calibration function. Changes that can obtained in one hot wire signal can in some cases not be seen in the corresponded resistance wire and vice versa. The non-agreement can be clear obtained when the hot wire signal directly after the shock stays on some what a constant value for some time, this behavior can not be seen

for the resistance wire, see figure 7.18. These non-agreements in registration of the flow properties together with that the resistance wire probably responds slower makes the calibration function invalid in some time sequences. What could happens for instance is that a high voltage from the hot wire occurs in the same time when the temperature is high that means that the velocity produced by the hot wire calibration function could go to extremely high values. To avoid these kind of problems the hot wire calibration function has only been applied for chosen parts of the signal trying to compare with the result from section 7.3. Something else that causes problem is when the temperature reaches very high temperatures, then you are so near the wire temperature that the extrapolation of the calibration function works too bad which will results in very high velocity values.

Looking at the experiment gas generator 4, second case, there is a very clear voltage plateau in the voltage signal, see figure 7.17 . Using this value together with temperature which is around 50 $[^{\circ}C]$ in the calibration function for the hot wire it turned out to be 46 $\frac{m}{s}$, but when the velocity is computed from the the unsteady shock wave theory it becomes 82 $\frac{m}{s}$. (Do not be confused by the little bump in the beginning of the temperature raise, this is a periodic disturbance coming up, but when the air/gas transition occur it is supposed to be gone.) As can be seen from the temperature profile the air/gas transition occurs around six ms, which is in the beginning of the plateau of the hot wire signal. One strange discover is that the hot wire signal does not show any sign on that a high temperature increase is coming. First after eight ms some events appears in the signal, high fluctuations and a decrease in voltage due to higher gas temperature are obtained, which is a reasonable appearance. Another strange behavior is the dip in the temperature time series which almost goes to zero after its firs great raise. The explanation could be reflected expansion waves, or the flow itself that occurs it. However, this is also a behavior that does not appear in the hot wire signal.

A similar data collection is obtained in case 3 experiment gas generator 6, where the air/gas transition appear in the beginning on the plateau in the hot wire signal. By doing the same procedure as above the velocity after the shock wave become 35 $\frac{m}{s}$ compared to the value computed from the the unsteady shock wave theory, 71 $\frac{m}{s}$ see figure 7.18. Using the hot wire data for the entire plateau and the corresponding temperature from resistance wire CW1 the velocity is computed using the hot wire calibration function, in figure 7.19 the velocity is shown. Mass flow calculations have also been made for the same time series, figure 7.20. Speed and mass flow time series are also shown for gas generator 7 & 10, figure 7.21, 7.22, 7.23 & 7.24. For gas generator 10 one longer speed and mass flow time series shown just to exemplify how the speed starts to behave unrealistic for higher temperatures, figure 7.25 & 7.26.

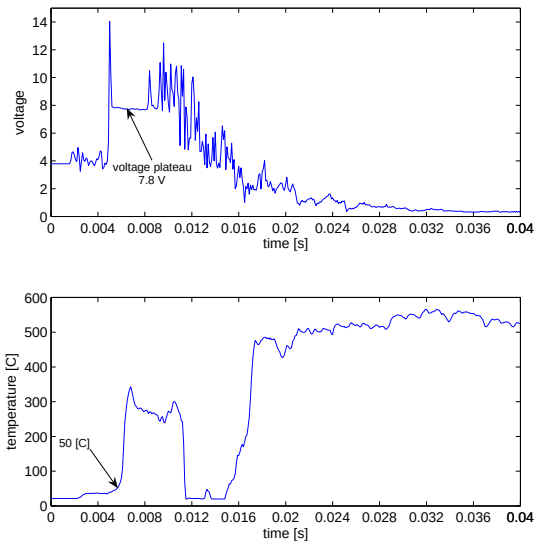


Figure 7.17: Hot wire signal on the top. Corresponding cold wire signal on the bottom, gas generator 4

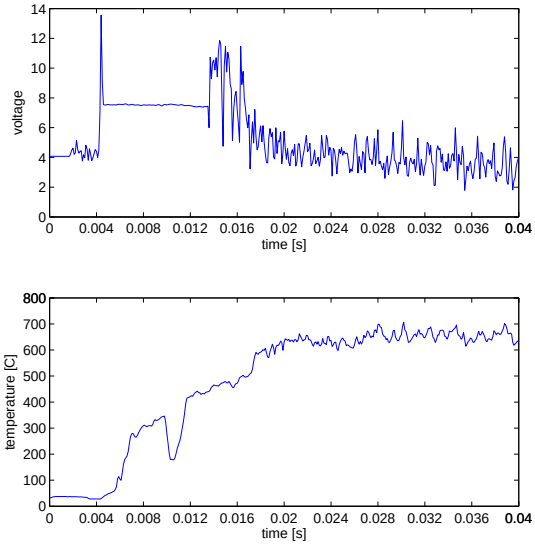


Figure 7.18: Hot wire signal on the top. Corresponding cold wire signal on the bottom, gas generator 6.

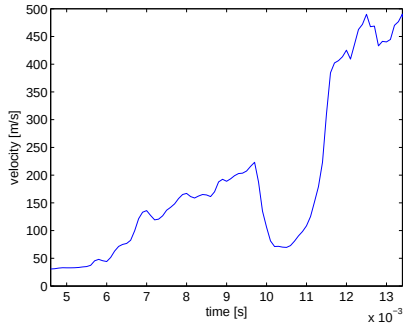


Figure 7.19: Speed at the plateau generated from the calibration function, Gas generator 6.

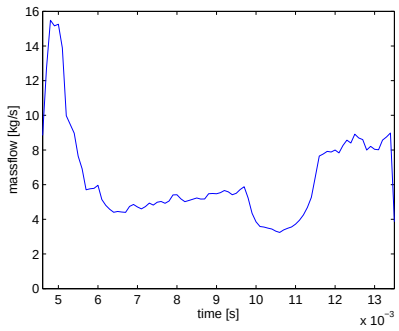


Figure 7.20: Mass flow at the plateau, Gas generator 6.

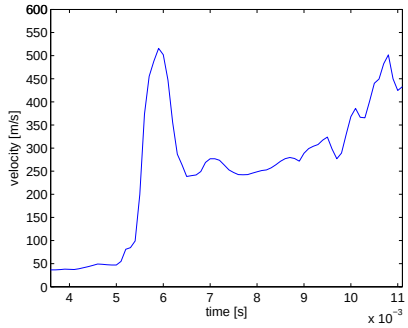


Figure 7.21: Speed at the plateau generated from the calibration function, Gas generator 7.

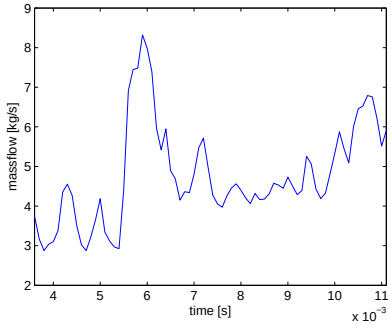


Figure 7.22: Mass flow at the plateau, Gas generator 7.

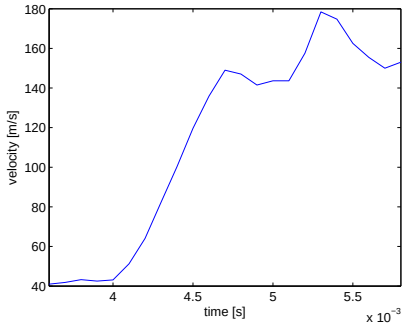


Figure 7.23: Speed at the plateau generated from the calibration function, Gas generator 10.

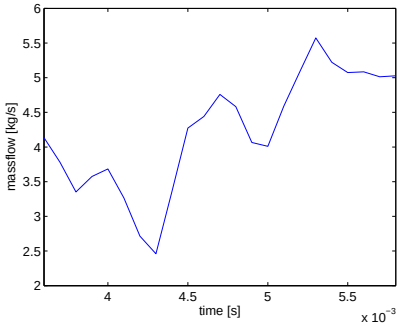


Figure 7.24: Mass flow at the plateau, Gas generator 10.

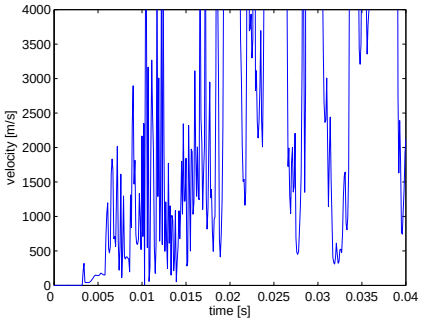


Figure 7.25: Speed at a longer time series generated from the calibration function, Gas generator 10.

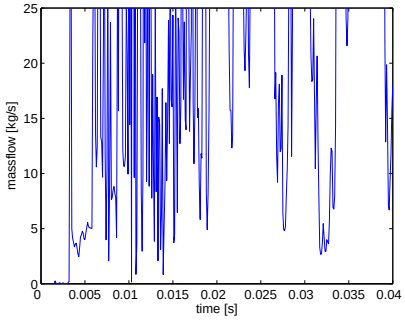


Figure 7.26: Mass flow at a longer time series, Gas generator 10.

7.5 Analysis of the first milliseconds

Since there occurs strange thing in the interval some where between 0.07 ms and 0.17 ms in both hot- and cold wire this part of the signal has to be analyzed. Considering the temperature which either show a large dip or a small dip or a kind of plateau in the signal. This events have a too long time duration to be explained by reflecting shock waves inside the cylindrical extension. More realistic is that it occurs a sudden expansion when the bag sudden yield, depending on how the bag is folded and fixed, which should result in a temperature decrease. This decrease should correspond to a pressure drop, by using the expression for isentropic expansion, 7.4.

$$\frac{P_1}{P_2} = \left(\frac{T_1}{T_2}\right)^{\gamma/(\gamma-1)} \tag{7.4}$$

In the pressure series it should therefore be possible to see even a larger decrease. But it could not be observed. Also the theory that flow from the outside has been sucked in through the probe holes, but this theory was discard when studying the movie of the inflation where it was clear that gas only went out from the holes. The only theory left that could explain the events is the gas generator itself which gives a uneven flow. Looking at the temperature plots in figure 7.2 & 7.2 they show very similar behavior of the flow from probe to probe for the same gas generator but the time series shows clear differences

from gas generator to gas generator.

Chapter 8

future work

There are many things that could be improved if another experiment is going to be done. The method used in this project could be improved by changing the calibration setup. The calibration set up had the lack of not having a wide calibration range considering both temperature and velocity. Limitations belonged to the heat gun which could not give neither high temperature or velocity but also not a non-fluctuating which made the data assembling more complicated, moreover the limitations also belonged to the probes and then specially to the tungsten wire which could not withstand more than 300 - 400 degrees Celsius. The absence of a calibration device which could vary all three parameters, velocity, temperature and pressure makes the hot wire calibration weak. For instance it was troublesome to extrapolate to higher temperatures for the hot wires. So an improvement of the calibration and thus the experiment itself is to use the calibration set up described in Sigfrids (2003) where velocity and the static pressure could be changed in a wide range with some modifications so it also can generate a high temperature flow. That presupposes that the pressure is measured in the experiment somewhat close to the probe which perhaps causes problem. When the calibration is of very accurate sort the dual hot wire technique would be interesting to apply in order to better the time response for the temperature measurements. The temperature measurements could be improved if the resistance wire could be able to withstand higher temperature so it will be possible not to extrapolate so far in the calibrations and they will also be improved by a more temperature stable flow so the temperature readings from the thermocouple will be more exact. To get a wider calibration range problems occurs when the tungsten wire can not stay long time in a too heat flow without getting damage. And a platinum - iridium wires only available as 10 μm which makes less response fast. However, the time response of a resistance wire, which is comparatively low to the hot wire, could be time compensated using the theory that the time constant only depends on the velocity. So the velocity obtained from the hot wire could be used to compute the time constant which can be used to correct the value from the resistance wire. But the hot wire need the temperature to be compute the velocity so this is a kind of iterative process. Probably it is a difficult task to manage. More about time compensation processes can be read in, Vukoslavcevic & James M Wallace (????) & Bremhorst & Graham (1990). Another method that would be interested to apply in this flow case is the aspirating probe which can give the temperature in the time response that the hot wires respond. To investigate weather the dips in the resistance wire signal or the plateau in the hot wire signal causes of reflecting

expansion waves or if it is the flow itself that causes it Schlieren technique would be a very useful tool to see shock waves and expansion waves will be visible, presupposed that the cylindric extender is made of a transparent material for example glass.

Finally, maybe not an improvement but certainly something that is interesting to see if it work, the optical technics especially the CARS technique. It has a high potential with very high resolution.

Bibliography

Anderson, J. J. D. 1990 *Modern Compressible Flow with historical perspective*. McGraw-Hill Publishing Company, ISBN 0-07-100665-6.

Bremhorst, K. & Graham, L. J. W. 1990 A fully compensated hot/cold wire anemometer system for unsteady flow velocity and temperature measurements. *Meas. Sci. Technol.* **1**, 425–430.

Bruun, H. H. 1995 *Hot-Wire anemometry*. Oxford University Press, Oxford, UK, ISBN 0-19-856342-6.

Childs, P. R. 2001 *Practical temperature measurements*. Butterworth-Heinemann, ISBN 0 7506 5080 X.

Christiansen, W. H. 1961 Development and calibration of a cold wire probe for use in shock tubes. Phd thesis. California Institute of Technology.

E. K. Gustafson, J. M. & Byer, R. ???? Development of a global interferometer skin-friction meter .

Incropera, F. P. 1981 *Fundamentals of heat and mass transfer*. John Wiley & Sons, Inc, 84-15272.

John C. LaRue, T. D. & Gibson, C. H. 1975 Measurements of high-frequency turbulent temperature. *Rev.Sci.Instrum.* **46**, 757–764.

Lomas, C. G. 1986 *Fundamentals of Hot wire Anemometry*. Cambringe University Press, 0 521 30340 0.

Ng, W. F. & Epstein, A. 1983 High-frequency temperature and pressure probe for unsteady compressible flows. *Rev.Sci.Instrum.* **54**, 1678–1683.

Sigfrids, T. 2003 Hot wire and piv studies of transonic wall-bounded flows. Licentiate thesis. Royal Institute of Technology Departments of Mechanics.

Vukoslavcevic, P. V. & James M Wallace, T. . ???? .